Sports Biomechanics

Assessment of planarity of the golf swing based on the functional swing plane of the clubhead and motion planes of the body points

Young-Hoo Kwon [a] , Christopher S. Como [a] , Kunal Singhal [a] ,
Sangwoo Lee [a] & Ki Hoon Han [a]

[a] Biomechanics Laboratory, Texas Woman's University, Denton, TX,
USA

Available online: 12 Mar 2012

First

PLEASE SCROLL DOWN FOR ARTICLE

Routledge
Taylor & Francis Group

Assessment of planarity of the golf swing based on the functional swing plane of the clubhead and motion planes of the body points

YOUNG-HOO KWON, CHRISTOPHER S. COMO, KUNAL SINGHAL, SANGWOO LEE, & KI HOON HAN

Biomechanics Laboratory, Texas Woman's University, Denton, TX, USA

Abstract
The purposes of this study were (1) to determine the functional swing plane (FSP) of the clubhead and the motion planes (MPs) of the shoulder/arm points and (2) to assess planarity of the golf swing based on the FSP and the MPs. The swing motions of 14 male skilled golfers (mean handicap = -0.5 ± 2.0) using three different clubs (driver, 5-iron, and pitching wedge) were captured by an optical motion capture system (250 Hz). The FSP and MPs along with their slope/relative inclination and direction/direction of inclination were obtained using a new trajectory-plane fitting method. The slope and direction of the FSP revealed a significant club effect ($p < 0.001$). The relative inclination and direction of inclination of the MP showed significant point ($p < 0.001$) and club ($p < 0.001$) effects and interaction ($p < 0.001$). Maximum deviations of the points from the FSP revealed a significant point effect ($p < 0.001$) and point–club interaction ($p < 0.001$). It was concluded that skilled golfers exhibited well-defined and consistent FSP and MPs, and the shoulder/arm points moved on vastly different MPs and exhibited large deviations from the FSP. Skilled golfers in general exhibited semi-planar downswings with two distinct phases: a transition phase and a planar execution phase.

Keywords: *Spiral, slope, direction angle, inclination, trajectory-plane fitting, semi-planar*

Introduction

Shot accuracy and consistency, in terms of direction and distance, are fundamental elements of performance in golf. Club motion during the downswing is an important aspect of the golf swing since shot direction and ball carry distance are largely determined by the impact conditions (clubhead velocity, clubface orientation, and impact location on the clubface). Hogan and Wind (1957) first used the term 'swing plane,' a widely used but controversial term in golf coaching lately, in their book titled *Ben Hogan's five lessons: The modern fundamentals of golf*. Their visualization of swing plane as a glass pane connecting the ball and the shoulder line with golfer's head sticking out through a hole in the pane, however, has caused misconceptions and been subject to criticism by other professionals (e.g. Haney & Huggan, 1999). More recent swing models that have gained popularity include Hank Haney's 'On-Plane' swing and Jim Hardy's 'One-Plane' and 'Two-Plane' swings

(Haney & Huggan, 1999; Hardy & Andrisani, 2005). None of these, however, has been mechanically scrutinized through scientific research.

For over 40 years, a large number of studies on swing mechanics have been conducted based on the double-pendulum swing model (e.g. Williams, 1967; Cochran & Stobbs, 1968; Lampsa, 1975; Budney & Bellow, 1979; Milburn, 1982; Milne & Davis, 1992; Sanders & Owens, 1992; Pickering & Vickers, 1999) or its triple-pendulum sibling (e.g. Sprigings & Neal, 2000; Sprigings & Mackenzie, 2002). The main features of the double-pendulum model include (a) the golfer is considered as a system of two levers hinged at the wrists/hands, (b) the upper lever corresponds to the golfer's shoulders and arms while the club forms the lower lever, and (c) the system is swung around a fixed point (hub) in a 'single inclined plane.' The multi-pendulum models have been particularly popular in modeling/simulation studies due to their simplicity. Although some modifications have been introduced, such as flexible clubshaft (Milne & Davis, 1992), triple pendulums (Campbell & Reid, 1985; Sprigings & Neal, 2000; Sprigings & Mackenzie, 2002), and moving hub (Jorgensen, 1994), the fundamental assumption of the model (i.e. the levers move in single inclined plane) remains unaltered.

Vaughan (1981), however, reported that the motion plane (MP) of the club was not planar by assessing the continuous motion of the clubshaft plane during the downswing. Neal and Wilson (1985) also concluded that motion of the club was not planar for any substantial period of time during the downswing. Coleman and Rankin (2005) systematically demonstrated that during the downswing the instantaneous left-arm plane (formed by left arm and shoulder line) continuously changed its orientation (inclination and direction), and the deviation of the clubhead from the left-arm plane was inconsistent. Coleman and Anderson (2007) further investigated the validity of planar swing by identifying a single swing plane that best fitted to the clubshaft motion with large mean goodness-of-fit values reported for all clubs used (driver, 5-iron, and pitching wedge; root-mean-square (RMS) residuals > 8 cm). In a study utilizing a full-body multi-link three-dimensional (3D) model of the golfer's body, Nesbit (2005) showed that the downswing did not take place in a fixed plane and there were significant club pitch motions during the downswing.

Although it is evident from the findings of recent studies that the entire downswing plane is not planar (Coleman & Rankin, 2005; Nesbit, 2005; Coleman & Anderson, 2007), the notion of planar swing can still be a viable one. As the golfer-club system overall forms an open chain and the ultimate goal of the downswing is to develop a high velocity of the distal end (clubhead), a planar downswing is the simplest shape of motion that one can achieve. The downswing is a fast motion executed in less than 260 ms (Cochran & Stobbs, 1968; Milburn, 1982; Neal & Wilson, 1985; Burden et al., 1998) and it is highly likely that a simpler downswing leads to more consistent and accurate shots. The swing plane can also effectively characterize a golfer's downswing, if such a plane indeed exists. Most of the impact conditions (clubhead velocity and impact location on the clubface) are directly associated with the properties of the swing plane so the swing plane can be a useful tool in assessing a golfer's fundamental swing motion. A critical review of literature on swing mechanics yields two observations. First, although the clubshaft plane (Vaughan, 1981; Neal & Wilson, 1985; Haney & Huggan, 1999; Coleman & Anderson, 2007) and postural planes (arm and shoulder planes; Coleman & Rankin, 2005; Hardy & Andrisani, 2005) have mainly been used in the argument of the planarity, what actually impacts on the ball is the clubhead, suggesting that the clubhead motion must be the primary focus in the definition of the swing plane. Second, when the anatomical structures and joint motions of the body (trunk and arms) during the downswing are considered, it is unrealistic to expect a single planar swing plane for the entire downswing. Rather, it is the plane formed by the clubhead near the

impact point, the 'functional swing plane' (FSP), that is of utmost importance. Therefore, a reassessment of the swing planarity based on this new definition of swing plane may shed light on and provide new insight into the complex 3D golf swing mechanics.

Moreover, due to the overwhelming popularity of the multi-pendulum models for over 40 years, the complex 3D motions of the shoulder/arm points that form the pendulums have been practically ignored and, consequently, not well understood. Simple (planar) motions of the pendulum points (shoulder/arm joints) are a prerequisite of a simple clubhead motion but to date no attention has been given to the complexity and nature of the motions of these points with respect to the swing plane. While it is evident from the recent findings that these body points do not move in a single inclined plane, it is important to investigate whether these points also form simple MPs of their own and how these MPs are positioned with respect to the swing plane formed by the clubhead. The purposes of this study were (1) to determine the FSP of the clubhead and the MPs of the pendulum points that characterize a golfer's fundamental downswing motion and (2) to systematically assess planarity of the golf swing based on the FSP and the MPs. It was hypothesized that (a) skilled golfers would exhibit well-defined and consistent FSPs during the downswing, and the properties of the FSP (planarity, slope, and direction) would be affected by the club used (driver, 5-iron, and pitching wedge), (b) skilled golfers would exhibit well-defined and consistent MPs of the shoulder/arm joints during the downswing, and the properties of the MPs (planarity, and relative inclination and direction of inclination with respect to the FSP) would vary among the points and be affected by the club used, and (c) the deviations of the shoulder/arm points from the FSP during the entire swing would vary among the points and be affected by the club used.

Methods

Participants

Fourteen right-handed male golfers were recruited from the North Texas area (Dallas, USA, and vicinity) for this study. The mean mass, height, age, and handicap were 83.8 ± 11.1 kg ($62.4-98.1$ kg), 180.5 ± 5.3 cm ($173.0-191.4$ cm), 32.8 ± 10.7 years ($19-50$ years), and -0.5 ± 2.0 (two 3-handicappers and 12 scratch-or-betters; plus handicaps were entered as negative numbers), respectively. Participants were free of serious muscular or joint/ligament problems within 6 months prior to the study. Ethics approval was secured from the Texas Woman's University Institutional Review Board and informed consents were obtained from the participants prior to data collection.

Trajectory-plane fitting

A new trajectory-plane fitting method was developed and used in this study. The trajectory of a point of interest (clubhead, hand, or shoulder; Q in Figure 1) can be fit to a plane defined by a point (P) whose position vector ($\mathbf{r}_o$) is normal to the plane (Figure 1)

$$\mathbf{r}_o = [x_o, y_o, z_o], \tag{1}$$

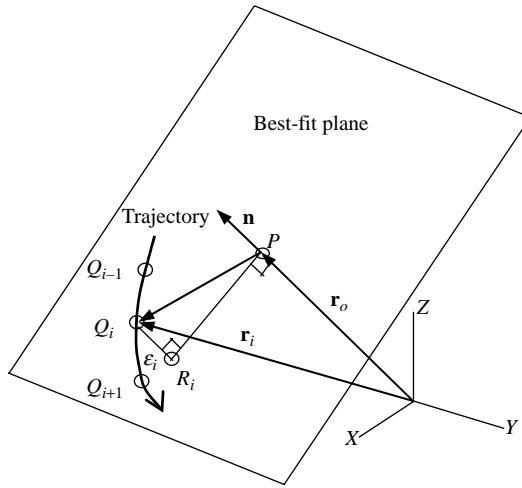$$\mathbf{n} = \frac{\mathbf{r}_o}{|\mathbf{r}_o|}, \tag{2}$$

Figure 1. The position ($\mathbf{r}_o$) and orientation ($\mathbf{n}$) of the best-fit trajectory plane can be described by a point on the plane (P) whose position vector is perpendicular to the plane. $\mathbf{n}$ is the unit vector of $\mathbf{r}_o$. R_i is the foot of trajectory point Q_i on the plane.

where $\mathbf{n}$ is the unit vector of $\mathbf{r}_o$. Random deviation of a given trajectory point from the plane (ε_i) can then be expressed as a function of $\mathbf{n}$

$$\varepsilon_i = (\mathbf{r}_i\text{-}\mathbf{r}_o)\cdot\mathbf{n}, \tag{3}$$

where $\mathbf{r}_i$ is the position of Q_i. Three trajectory points or more provide a sufficiently determined nonlinear system of equations

$$\mathbf{F} = \begin{bmatrix} w_1\varepsilon_1 \\ \cdot \\ w_i\varepsilon_i \\ \cdot \\ w_m\varepsilon_m \end{bmatrix} \approx 0, \tag{4}$$

where w_i is the scalar weight and m is the point count (≥ 3); m is a function of the sampling frequency and the phase of swing from which the trajectory is extracted. From Equation (4), the Jacobian matrix can be derived

$$\mathbf{J} = \begin{bmatrix} w_1\dfrac{\partial \varepsilon_1}{\partial x_o} & w_1\dfrac{\partial \varepsilon_1}{\partial y_o} & w_1\dfrac{\partial \varepsilon_1}{\partial z_o} \\ \cdot & \cdot & \cdot \\ w_i\dfrac{\partial \varepsilon_i}{\partial x_o} & w_i\dfrac{\partial \varepsilon_i}{\partial y_o} & w_i\dfrac{\partial \varepsilon_i}{\partial z_o} \\ \cdot & \cdot & \cdot \\ w_m\dfrac{\partial \varepsilon_m}{\partial x_o} & w_m\dfrac{\partial \varepsilon_m}{\partial y_o} & w_m\dfrac{\partial \varepsilon_m}{\partial z_o} \end{bmatrix}, \tag{5}$$

where the partial derivatives assume the following form:

$$\left[\frac{\partial \varepsilon_i}{\partial x_o}, \frac{\partial \varepsilon_i}{\partial y_o}, \frac{\partial \varepsilon_i}{\partial z_o}\right] = \frac{1}{(\mathbf{r}_o \cdot \mathbf{r}_o)^{1/2}}(\mathbf{r}_i\text{-}2\mathbf{r}_o)\text{-}\frac{(\mathbf{r}_i\text{-}\mathbf{r}_o)\cdot\mathbf{r}_o}{(\mathbf{r}_o\cdot\mathbf{r}_o)^{3/2}}\mathbf{r}_o. \tag{6}$$

The Newton–Raphson method (Press et al., 2002) was applied to Equations (4)–(6) to solve the system for $\mathbf{r}_o$. Since trajectory points were sampled at a constant frequency, their spatial density varied as a function of point speed. Thus, a homogeneous trajectory point distribution was achieved by using the speed of the trajectory point as weight in Equations (4) and (5). This trajectory-plane fitting method allowed investigators to overcome the main shortcoming of the regression-based method (Coleman & Rankin, 2005; Coleman & Anderson, 2007) in which only the vertical coordinates of the trajectory points were subject to fitting.

Planarity of the trajectory, how well the trajectory fits to the plane, was assessed by the RMS and maximum fitting errors

$$\varepsilon_{\text{RMS}} = \sqrt{\frac{1}{\sum\limits_{i=1}^{m}w_i}\sum_{i=1}^{m}w_i[(\mathbf{r}_i\text{-}\mathbf{r}_o)\cdot\mathbf{n}]^2}, \tag{7}$$

$$\varepsilon_{\text{max}} = \max(|(\mathbf{r}_i\text{-}\mathbf{r}_o)\cdot\mathbf{n}|). \tag{8}$$

A smaller error measure (in cm) means a more planar trajectory.

Club conditions

Three clubs were used: driver, 5-iron, and pitching wedge. Each participant used his own clubs and no attempt was made to control the club properties (weight, length, make, etc.). Each participant performed five successful trials with each club. The success of a shot was determined by shot direction, launch angle, and golfer's input in terms of solidness of the impact and body motion. Sufficient practice shots were allowed for acclimatization prior to data collection with each club.

Experimental setup

A 250-Hz 10-camera VICON motion capture system (Centennial, CO, USA) was used in an indoor motion analysis laboratory to capture the 3D coordinates of the retro-reflective markers (~10-mm diameter) attached on the golfer's body and club. The full 'TWUGolfer' marker set (Figure 2; Table I) was used for the analysis and detailed graphical presentation of the body motion. A total of 65 markers were utilized in four different types of trials captured in each club condition: a ball–plate trial (Figure 2A), a club trial (Figure 2B), a static posture trial (Figure 2C), and motion trials (Figure 2D). The ball–plate, club, and static posture trials were used in locating a group of markers removed in the motion trials for non-obstructed swing (Figure 2E; Tables I and II). Participants were asked to put on black spandex shirts/shorts for the motion capture purposes.

Practice foam balls were used instead of actual golf balls in the motion trials. The ball mat (30 × 60 cm) was placed at the center of the laboratory with a vertical target line marked on the front wall located 10.6 meters away from the mat. The Y-axis of the
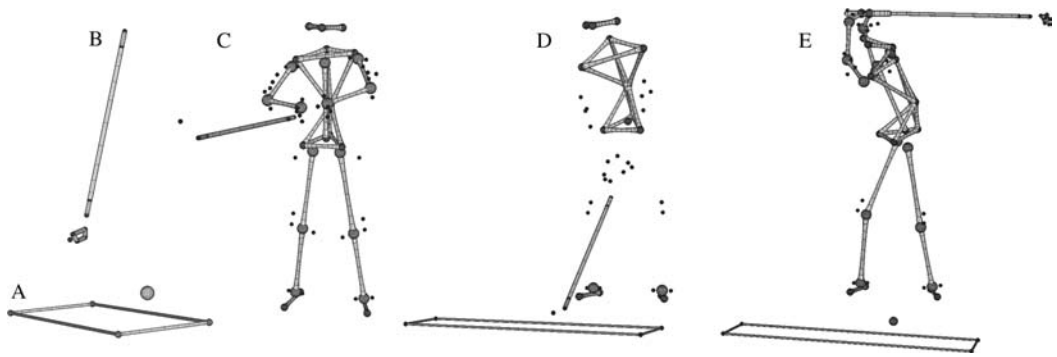
Figure 2. Different types of trials utilized: (A) ball–plate trial, (B) club trial, (C) static posture trial, (D) unprocessed motion trial, and (E) processed motion trial.

laboratory reference frame was aligned with the direction of target with the Z-axis being vertical. Golfers were facing in the direction of the positive X-axis at address. In the driver condition, two different tee heights were used (3.9 and 5.4 cm above the mat surface) and participants were allowed to choose their preferred height. The surfaces of the hitting box and the mat were leveled.

Trial processing

Captured marker coordinates (250 Hz) were imported into Kwon3D Motion Analysis Suite (Version XP, Visol Inc., Seoul, Korea) for subsequent data processing and analysis. The raw coordinates were filtered using a Butterworth zero phase-lag fourth-order low-pass filter with a cut-off frequency of 20 Hz. The ball–plate, club, and static posture trials collected in each club condition were combined with the motion trials to locate the markers removed in the motion trials (Figures 2A–2E). The 89-point 'TWUGolfer' body model was used in this process (Table I) in which a group of points (24 computed points including 13 joint centers) were derived additionally from the markers to facilitate analysis. (See Tables I and II for details of the computed points.)

To improve the time resolution for more accurate event detection, the processed point position data were up-sampled to 2000 Hz using cubic spline-based interpolation. Eight events were identified based on the clubshaft position: take-away (TA), mid backswing (MB), late backswing (LB), top of backswing (TB), early downswing (ED), mid downswing (MD), ball impact (BI), and mid follow-through (MF; Figure 3).

Data analysis

Determination of the FSP and MPs. Trajectory-plane fitting was carried out for the clubhead in three different phases: TB–MF (Figure 4A), ED–MF (Figure 4B), and MD–MF (Figure 4C). The RMS and maximum trajectory fitting errors (Equations (7) and (8)) were compared among these phases to identify the phase which provided sufficiently well-defined FSPs. The best-fit planes obtained from this particular phase were used as the FSPs in subsequent analyses. The slope of the FSP (ϕ_{FSP}) was computed as the angle between the ground and the FSP, whereas the angle between the intersection line formed by the FSP with the ground ($\mathbf{d}_{FSP}$) and the Y-axis (direction of the target) was used as

Table I. The 89-point (65-marker) 'TWUGolfer' body model/marker set.

Section	Markers/computed points used	
Ball–Plate	Markers (5)	Static ball marker and four corner markers (Figure 2A). The static ball marker was removed in the motion trials (Figures 2D) but located indirectly in conjunction with the ball–plate trial using the 'Rigid Body Method' (see Table II).
Markers (9)	Markers (9)	Five shaft/head markers and four clubface markers (Figure 2B). The clubface markers were removed in the motion trials (Figure 2D) but located indirectly from the three distal markers in conjunction with the club trial using the 'Rigid Body Method' (see Table II).
Computed (5)	Computed (5)	Right- and left-hand centers, mid-hand, grip end, and clubhead (Figure 2E). Hand centers and end of grip were computed from the two proximal shaft markers using the 'Unit Vector Method' (see Table II). Mid-hand is mid-point of the hand centers. The clubhead position is the arithmetic mean of the clubface marker positions.
Pelvis	Markers (3)	Three pelvic markers: right and left anterior superior iliac spines (ASISs) and sacrum.
	Computed (5)	Mid-ASIS, L4/L5, hip joints, and mid-hip. Mid-ASIS is mid-point of the anterior superior iliac spine markers (right and left ASISs). The L4/L5 joint was located using the 'MacKinnon Method' while the hip joint centers were computed using the 'Tylkowski-Andriacchi Method' (see Table II). Mid-hip is the mid-point of the hip joints.
Trunk	Markers (4)	Four trunk markers (right and left acromions, C7, and T12)
	Computed (1)	Mid-shoulder. Mid-shoulder is mid-point of the shoulder joint centers.
Legs	Markers (8 × 2)	Four thigh markers each (greater trochanter, lateral thigh, and lateral and medial epicondyles), two shank markers each (lateral and medial malleoli), and two foot markers each (toe and heel). The greater trochanter marker and the medial femoral epicondyle marker were removed in the motion trials (Figure 2D).
	Computed (2 × 2)	Knee joints and ankle joints. The knee joint center was located indirectly in the motion trials (Figure 2E) using the 'Extended Mid-Point Method' (see Table II). The ankle joint center is mid-point of the lateral and medial malleoli.
Arms	Markers (12 × 2)	Seven upper arm markers each (anterior and posterior shoulders, three upper arm markers, and medial and lateral epicondyles), two forearm markers each (radial and ulnar styloid processes), and three hand markers each. The anterior/posterior shoulder markers, medial humeral epicondyle marker, and the ulnar styloid marker were removed in the motion trials (Figure 2D).
	Computed (3 × 2)	Shoulder, elbow, and wrist joints. The shoulder, elbow, and wrist joint centers were located indirectly in the motion trials using the 'Extended Mid-Point Method' (see Table II).
Head	Markers (4)	Four head markers (right, left, forehead, and vertex)
	Computed (1)	Head center. Head center is mid-point of the right and left head markers.
Swing plane	Computed (2)	Projected clubhead and instantaneous rotation center. Clubhead was projected to the FSP to obtain the projected clubhead position. From the curvature of the projected clubhead trajectory, the instantaneous rotation centers were computed.

Table II. Methods used in locating the computed points.

| Method	Description
Rigid body	In this method, location of the point of interest (the unknown point whose position is known in the static posture trial but unknown in the motion trial) was computed from the motion of a group of points commonly observed in both trials (the common points; three or more). Translation and rotation of the rigid body formed by the common points were quantified and applied to the unknown point to obtain its position in the motion trial. The static ball and clubface marker positions were obtained using this method with the ball–plate corner markers and the markers placed on the distal end of the club being the common points, respectively (Williams & Sih, 2002). This method was also utilized in the 'Extended Mid-Point Method' (see below).
Unit vector	Hand centers and end of grip were computed based on the unit vector defined by two markers on proximal shaft near the grip and the measured distances to these points from the grip marker. For the hand centers, the grip marker-to-middle finger distance was used.
MacKinnon	In the static posture trial, the L4/L5 joint position was computed following the method outlined by MacKinnon and Winter (1993) based on three pelvic markers (right and left ASISs and sacrum). The joint position was then described relative to the pelvis reference frame defined by the pelvic markers. In the motion trials, this local position was used in locating the L4/L5 joint.
Tylkowski–Andriacchi	In the static posture trial, the hip joint position was computed following the method outlined by Bell et al. (1990), a hybrid of the methods of Tylkowski et al. (1982) and Andriacchi et al. (1980), based on the pelvic markers and the greater trochanter marker. The hip joint position was then described relative to the pelvis reference frame defined by the pelvic markers. In the motion trials, this local position was used in locating the joint thus eliminating the need for the greater trochanter marker.
Extended mid-point	In the static trial, the joint center position was computed as the mid-point of the lateral and medial joint markers (anterior and posterior markers in the case of shoulder). In the motion trials, the medial marker (both the anterior and posterior markers in the case of shoulder) was removed for obstruction-free performance and the 'Rigid Body Method' was used to locate the joint center with the joint being the unknown point and $3+$ markers attached to the segment as the common points. For the shoulder and elbow joints, the three upper arm markers were used as the common points, whereas the three hand markers on the dorsal side were used for this purpose for the wrist joint.
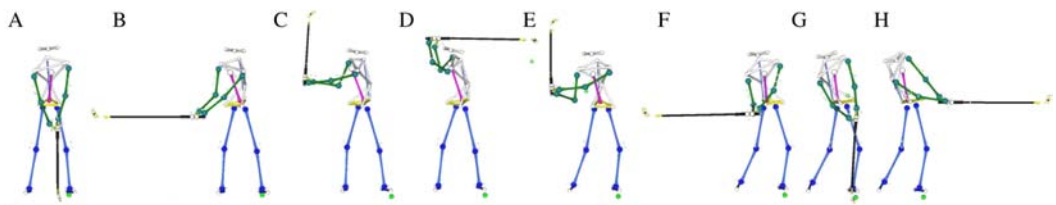
Figure 3. Golf swing events: (A) take-away, (B) mid backswing, (C) late backswing, (D) top of backswing, (E) early downswing, (F) mid downswing, (G) ball impact, and (H) mid follow-through.
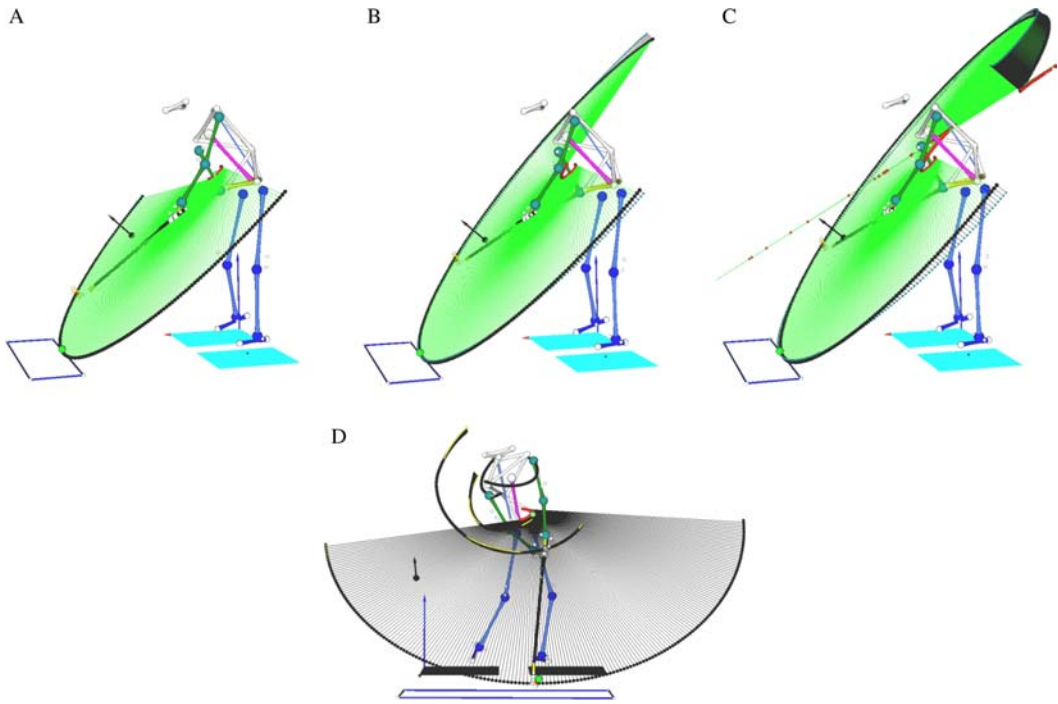
Figure 4. The best-fit trajectory planes of the points: (A) clubhead for the MD–MF phase, (B) clubhead for the ED–MF phase, (C) clubhead for the TB–MF phase, and (D) the shoulder/arm points for the TB–MF phase. Abbreviations: MD, mid downswing; ED, early downswing; TB, top of backswing; and MF, mid follow-through.
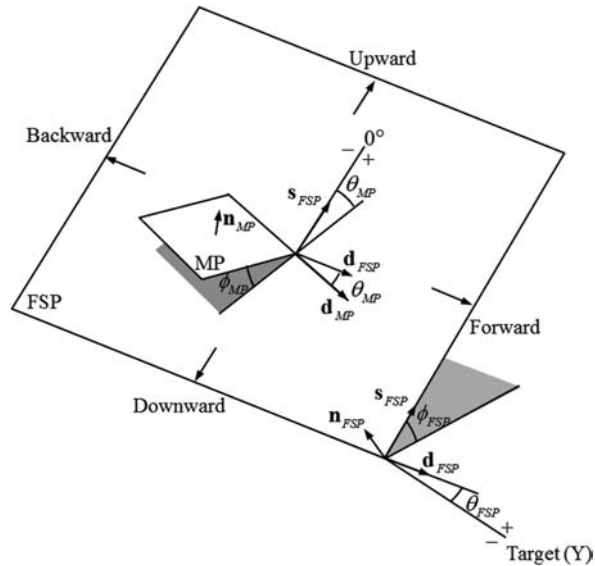
Figure 5. Orientations of the FSP and the MP. Shaded areas show the projections of the FSP on the ground and the MP on the FSP. $\mathbf{n}_{FSP}$, $\mathbf{d}_{FSP}$, and $\mathbf{s}_{FSP}$ are the normal, direction, and slope vectors of the FSP, respectively. $\mathbf{n}_{MP}$ and $\mathbf{d}_{MP}$ are the normal and direction vectors of the MP, respectively. The slope (ϕ_{FSP}) and direction angle (θ_{FSP}) of the FSP were computed relative to the ground and with respect to the Y-axis of the global reference frame, respectively. The relative inclination of the MP (ϕ_{MP}) was computed against the FSP. The direction of inclination of the MP (θ_{MP}) was computed with respect to the slope vector (-$\mathbf{s}_{FSP}$) of the FSP.

the direction angle (θ_{FSP}; Figure 5)

$$\phi_{FSP} = \cos^{-1}(\mathbf{n}_{FSP}\cdot\mathbf{k}), \tag{9}$$

$$\mathbf{d}_{FSP} = \frac{\mathbf{k}\times\mathbf{n}_{FSP}}{|\mathbf{k}\times\mathbf{n}_{FSP}|}, \tag{10}$$

$$\theta_{FSP} = \text{sign}(\mathbf{i}\cdot\mathbf{d}_{FSP})\cdot\cos^{-1}(\mathbf{j}\cdot\mathbf{d}_{FSP}), \tag{11}$$

where $\mathbf{i}$, $\mathbf{j}$, and $\mathbf{k}$ are unit vectors of the X-, Y- and Z-axes, respectively. An FSP directed to the left side of the target yielded a positive direction angle (Equation (11)).

Trajectory-plane fitting was carried out for the shoulders, right elbow, and the left-hand center in the TB−MF phase (Figure 4D). Since the left elbow remains extended during most part of the downswing, its trajectory is highly dependent on those of the left shoulder and hand and, for this reason, left elbow was excluded from plane fitting. Right hand was also excluded from plane fitting as its motion should be similar to that of the left hand. The orientations of the MPs were computed relative to the FSP, not to the ground/target line (Figure 5)

$$\phi_{MP} = \cos^{-1}(\mathbf{n}_{FSP}\cdot\mathbf{n}_{MP}), \tag{12}$$

$$\mathbf{d}_{MP} = \frac{\mathbf{n}_{MP}\times\mathbf{n}_{FSP}}{|\mathbf{n}_{MP}\times\mathbf{n}_{FSP}|}, \tag{13}$$

$$\theta_{MP} = \text{sign}(\text{-}\mathbf{s}_{FSP}\cdot\mathbf{d}_{MP})\cdot\cos^{-1}(\mathbf{d}_{FSP}\cdot\mathbf{d}_{MP}), \tag{14}$$

where ϕ_{MP} and θ_{MP} are the relative inclination and direction of inclination of an MP, respectively, $\mathbf{s}_{FSP}$ is the slope vector of the FSP, and $\mathbf{n}_{MP}$ and $\mathbf{d}_{MP}$ are the normal and direction vectors of the MP, respectively (Figure 5).

Off-plane motion patterns and maximum deviations of the pendulum points from the FSP. To obtain the off-plane motion patterns of the clubhead and shoulder/arm points during the swing, deviations of these points from the FSP were computed throughout the entire swing (TA−MF) phase using Equation (3). Ensemble averages were computed for the generalized off-plane motion patterns and the TA−MF time was used as 100% for time normalization. The maximum deviations from the FSP were computed in the TA−MF phase for the clubhead and the pendulum points using Equation (8).

Statistical analysis

A two-way (3×3) repeated measure MANOVA was carried out to compare the RMS/maximum trajectory fitting errors of the clubhead (two variables) among the PHASE conditions (within-subject factor; TB−MF, ED−MF, and MD−MF) and CLUB conditions (within-subject factor; driver, 5-iron, and pitching wedge). A one-way repeated measure MANOVA was conducted to compare the slope and direction angles of the FSP (two variables) among the CLUB conditions. The RMS/maximum trajectory fitting errors (two variables) of the MPs were compared among the POINT conditions (within-subject factor; left shoulder, left hand, right shoulder, and right elbow) and CLUB conditions using a two-

way (4×3) repeated measure MANOVA. An additional two-way (4×3) repeated measure MANOVA was used to compare the relative inclinations and directions of inclination of the MPs (two variables) among the POINT and CLUB conditions. A two-way (5×3) repeated measure ANOVA was used to compare the maximum deviations of the clubhead and shoulder/arm points among the POINT and CLUB conditions.

The Huynh–Feldt adjustment was carried out to correct for violation of circularity, if any. Post-hoc tests were carried out for each MANOVA/ANOVA with significant factor effect(s) and/or interaction. An alpha level of 0.05 was used in all statistical operations with appropriate adjustments (Bonferroni adjustment) for multiple comparisons. For each variable, the mean of the five trials performed by each participant in each club condition was computed and used in the MANOVAs/ANOVAs. The *SD* of the five trials in each club condition was used as the measure of intra-golfer variability (IGV) to assess the consistencies.

Results

Determination of the FSPs

The trajectory fitting errors (RMS and maximum) of the clubhead showed significant CLUB (Wilks' $\lambda = 0.474$, $F_{4,54} = 6.11$, $p < 0.001$, $\eta^2 = 0.312$) and PHASE (Wilks' $\lambda = 0.051$, $F_{4,54} = 46.44$, $p < 0.001$, $\eta^2 = 0.312$) effects and CLUB × PHASE interactions (Wilks' $\lambda = 0.338$, $F_{8,110} = 9.89$, $p < 0.001$, $\eta^2 = 0.418$). The errors were larger in the driver condition than in the 5-iron or pitching wedge conditions. The MD-MF phase provided well-defined best-fit planes with the mean maximum trajectory errors of approximately 0.9 cm in all three CLUB conditions (Table III). The best-fit planes obtained from this phase were used as the FSPs in subsequent analyses.

Slopes and direction angles of the FSPs

Slope and direction angles of the FSP revealed significant CLUB effect (Wilks' $\lambda = 0.001$, $F_{2,12} = 88.27$, $p < 0.001$, $\eta^2 = 0.999$). The slope decreased as the club length increased (Table III). The FSP tended to direct to the right side of the target (negative direction angle; closed plane) in the driver condition but to the left (positive direction angle; open plane) in the 5-iron and pitching wedge conditions. The mean IGV values of the slopes and direction angles of the FSPs were 1.0° or smaller in all CLUB conditions.

MPs of the shoulder/arm points

The trajectory fitting errors (RMS and maximum) of the pendulum points revealed significant POINT effect (Wilks' $\lambda = 0.176$, $F_{6,76} = 17.56$, $p < 0.001$, $\eta^2 = 0.581$) but insignificant CLUB effect (Wilks' $\lambda = 0.875$, $F_{4,50} = 0.87$, $p < 0.491$, $\eta^2 = 0.065$) and CLUB × POINT interaction (Wilks' $\lambda = 0.796$, $F_{12,154} = 0.113$, $p < 0.099$, $\eta^2 = 0.108$). The left hand and right elbow showed larger trajectory fitting errors than the shoulders (Table IV). The relative inclinations and directions of inclination of the MPs were collectively characterized by significant POINT (Wilks' $\lambda = 0.004$, $F_{6,76} = 196.86$, $p < 0.001$, $\eta^2 = 0.940$) and CLUB (Wilks' $\lambda = 0.297$, $F_{4,50} = 10.45$, $p < 0.001$, $\eta^2 = 0.455$) effects and significant POINT–CLUB interaction (Wilks' $\lambda = 0.288$, $F_{12,154} = 11.10$, $p < 0.001$, $\eta^2 = 0.464$). The CLUB effects were mainly observed in the direction of inclination measures (Table IV). In general, larger inter-golfer variability

Table III. Planarity of the clubhead trajectory and orientation of the functional swing plane (FSP; $n = 14$; $M \pm SD$).

		Driver		5-Iron		Pitching wedge		Sig. effects
		Group mean	(IGV)	Group mean	(IGV)	Group mean	(IGV)	
RMS error (cm)	TB to MF	5.6 ± 2.2	(0.4 ± 0.2)	4.6 ± 1.5[a]	(0.5 ± 0.4)	4.2 ± 1.3[a,b]	(1.6 ± 0.7)	PHASE
	ED to MF	1.3 ± 0.7[c]	(0.2 ± 0.1)	1.3 ± 0.7[c]	(0.2 ± 0.2)	1.4 ± 0.7[c]	(0.7 ± 0.4)	CLUB
	MD to MF	0.3 ± 0.2[c,d]	(0.1 ± 0.0)	0.3 ± 0.2[c,d]	(0.1 ± 0.1)	0.4 ± 0.2[c,d]	(0.2 ± 0.1)	PHASE × CLUB
Max error (cm)	TB to MF	23.5 ± 6.2	(1.3 ± 0.6)	19.5 ± 4.1[a]	(1.7 ± 1.3)	17.6 ± 4.2[a,b]	(0.4 ± 0.2)	
	ED to MF	4.8 ± 2.5[c]	(0.5 ± 0.3)	4.8 ± 2.5[c]	(0.8 ± 0.6)	5.2 ± 2.6[c]	(0.2 ± 0.1)	
	MD to MF	0.9 ± 0.6[c,d]	(0.2 ± 0.1)	0.9 ± 0.4[c,d]	(0.2 ± 0.1)	0.9 ± 0.5[c,d]	(0.1 ± 0.1)	
FSP slope (°)		47.2 ± 2.3	(0.5 ± 0.3)	55.8 ± 1.5[a]	(0.9 ± 0.5)	59.1 ± 1.9[a,b]	(0.7 ± 0.3)	CLUB
FSP direction (°)		-2.7 ± 3.6	(0.9 ± 0.4)	0.3 ± 3.2[a]	(1.0 ± 0.4)	0.1 ± 3.0[a]	(1.0 ± 0.4)	

Abbreviations: TB, top of backswing; ED, early downswing; MD, mid downswing; MF, mid follow-through; IGV, intra-golfer variability; [a] significantly different from the matching driver condition; [b] significantly different from the matching 5-iron condition; [c] significantly ($p < 0.05$) different from the matching TB–MF phase condition; [d] significantly different from the matching ED–MF phase condition.

Table IV. Planarity and orientation of the MPs of the shoulder/arm joints ($n = 14$; $M \pm SD$).

		Driver		5-Iron		Pitching wedge		Sig. effects
		Group mean	(IGV)	Group mean	(IGV)	Group mean	(IGV)	
RMS error (cm)	Left shoulder	0.4 ± 0.2	(0.0 ± 0.0)	0.4 ± 0.2	(0.1 ± 0.0)	0.4 ± 0.1	(0.1 ± 0.0)	
	Left hand[a]	1.7 ± 0.4	(0.2 ± 0.1)	1.5 ± 0.4	(0.2 ± 0.1)	1.5 ± 0.3	(0.1 ± 0.1)	
	Right shoulder[b]	0.4 ± 0.2	(0.0 ± 0.0)	0.4 ± 0.2	(0.0 ± 0.0)	0.3 ± 0.2	(0.1 ± 0.0)	
	Right elbow[a,c]	1.2 ± 0.8	(0.1 ± 0.1)	1.3 ± 0.6	(0.1 ± 0.0)	1.3 ± 0.5	(0.1 ± 0.0)	POINT
Max error (cm)	Left shoulder	1.2 ± 0.6	(0.2 ± 0.1)	1.0 ± 0.5	(0.2 ± 0.1)	1.0 ± 0.4	(0.2 ± 0.1)	
	Left hand[a]	5.0 ± 1.9	(0.6 ± 0.3)	4.3 ± 1.8	(0.6 ± 0.4)	4.2 ± 1.3	(0.4 ± 0.3)	
	Right shoulder[b]	1.1 ± 0.7	(0.2 ± 0.1)	1.0 ± 0.6	(0.2 ± 0.1)	1.0 ± 0.8	(0.2 ± 0.1)	
	Right elbow[a,b,c]	2.9 ± 1.3	(0.3 ± 0.1)	3.0 ± 1.6	(0.3 ± 0.2)	3.1 ± 1.2	(0.2 ± 0.1)	
Relative inclination (°)	Left shoulder	10.7 ± 4.3	(0.8 ± 0.3)	12.9 ± 4.5[d]	(1.1 ± 0.5)	15.0 ± 4.6[d,e]	(0.9 ± 0.4)	
	Left hand	11.3 ± 2.6	(0.6 ± 0.4)	10.8 ± 2.4	(0.6 ± 0.2)	10.2 ± 2.2[d,e]	(0.7 ± 0.4)	
	Right shoulder	29.8 ± 6.1[a,b]	(1.9 ± 1.2)	30.1 ± 5.6[a,b]	(1.8 ± 1.1)	31.0 ± 7.1[a,b]	(1.6 ± 0.8)	POINT
	Right elbow	38.5 ± 7.3[a,b,c]	(5.2 ± 3.3)	37.7 ± 7.0[a,b,c]	(1.9 ± 1.5)	37.2 ± 7.2[a,b,c]	(2.1 ± 1.5)	CLUB
Direction of inclination (°)	Left shoulder	67.6 ± 29.5	(1.4 ± 0.7)	38.4 ± 19.3[d]	(6.1 ± 4.1)	33.5 ± 13.8[d]	(5.7 ± 3.2)	POINT × CLUB
	Left hand	152.9 ± 22.7[a]	(3.7 ± 2.0)	143.6 ± 20.2[a,d]	(6.1 ± 4.8)	133.8 ± 20.7[a,d]	(7.2 ± 5.9)	
	Right shoulder	-75.7 ± 17.3[a,b]	(2.0 ± 1.1)	-75.7 ± 16.5[a,b]	(2.0 ± 1.0)	-76.9 ± 16.1[a,b]	(2.4 ± 1.3)	
	Right elbow	-107.5 ± 15.8[a,b,c]	(1.5 ± 0.7)	-105.3 ± 17.1[a,b,c]	(2.2 ± 0.9)	-104.1 ± 17.5[a,b,c]	(2.8 ± 1.5)	

Notes: A positive direction angle means that the MP is sloped toward the target. A negative value means that the MP is sloped away from the target (Figure 5). Abbreviation: IGV, intra-golfer variability; [a] significantly ($p < 0.05$) different from the matching left shoulder condition; [b] significantly different from the matching left hand condition; [c] significantly different from the matching right shoulder condition; [d] significantly different from the matching driver condition; [e] significantly different from the matching 5-iron condition.

and IGV values were observed in the directions of inclination than in the relative inclinations (Table IV).

Maximum deviation of the clubhead and shoulder/arm joints from the FSP

The ensemble average off-plane motion patterns (deviations from the FSP) of the clubhead and shoulder/arm points for the entire swing (TA–MF) are presented in Figure 6A–6C. Exemplar off-plane motion patterns of a golfer (driver condition only) are also presented in Figure 6D. In general, large deviations of the pendulum points from the FSP were observed. Maximum deviations revealed significant POINT effect ($F_{2.061} = 239.27$, $p < 0.001$, $\eta^2 = 0.948$) and POINT–CLUB interaction ($F_{2.734} = 35.60$, $p < 0.001$, $\eta^2 = 0.733$). The CLUB effect, however, was not significant ($F_{1.617} = 2.10$, $p = 0.154$, $\eta^2 = 0.139$). Clubhead and left shoulder were characterized by larger mean deviations from the FSP than others. Right elbow was identified as the point showing the smallest deviation from the FSP whose maximum deviation occurred below the FSP.

Discussion and implications

Functional swing plane

In all club conditions, skilled golfers exhibited well-defined and consistent FSPs in the MD–MF phase: (a) the mean RMS and maximum plane fitting errors were less than 1 cm for all clubs with the IGVs of the error measures being 0.2 cm or less and (b) the IGVs of the slopes and direction angles were 1° or less (Tables III). With the FSP clearly defined in the MD–MF phase, the downswing can be divided into two phases: the 'transition phase' (TB–MD) and the planar 'execution phase' (MD–MF). The downswing is not planar as a whole but planar in the execution phase that includes the most important event of the downswing, the impact. The impact conditions can be altered by adjusting the orientation of the FSP with respect to the target line and the orientation of the clubface relative to the FSP. The orientation of the FSP was affected by the club used: a longer club resulted in a flatter and more closed (in-to-out) FSP with respect to the target line (Table III).

Coleman and Anderson (2007) reported slopes and direction angles of the swing planes obtained from the motion of the clubshaft during the TB–BI phase: $54.5 \pm 3.0°$, $62.9 \pm 3.0°$, and $66.4 \pm 2.7°$ slopes, and $-7.8 \pm 5.9°$, $-4.9 \pm 5.7°$, and $-5.9 \pm 6.0°$ direction angles for driver, 5-iron, and pitching wedge, respectively. The slopes reported by these investigators were in general larger than those obtained in this study and the direction angles also showed more closed plane orientations (more negative). A direct comparison, however, was not possible due to the differences in the definitions of the swing plane. The RMS residuals reported (8.1 ± 2.4, 9.2 ± 3.2, and 10.6 ± 3.3 cm for driver, 5-iron, and pitching wedge, respectively) were substantially larger than those observed in this study and even larger maximum residuals were expected. These large residual values essentially suggest that the usefulness of the swing plane obtained from the shaft motion in the TB–BI phase is limited.

Motions of the body points

Although not as clean as the FSP, skilled golfers exhibited reasonably well-defined MPs of the shoulder/arm points: the mean RMS trajectory fitting errors were 1.7 cm or less while the mean maximum errors were 5.0 cm or less with the IGV of both error measures being 0.6 cm or less (Table IV). The left hand and right elbow revealed larger plane fitting errors than the
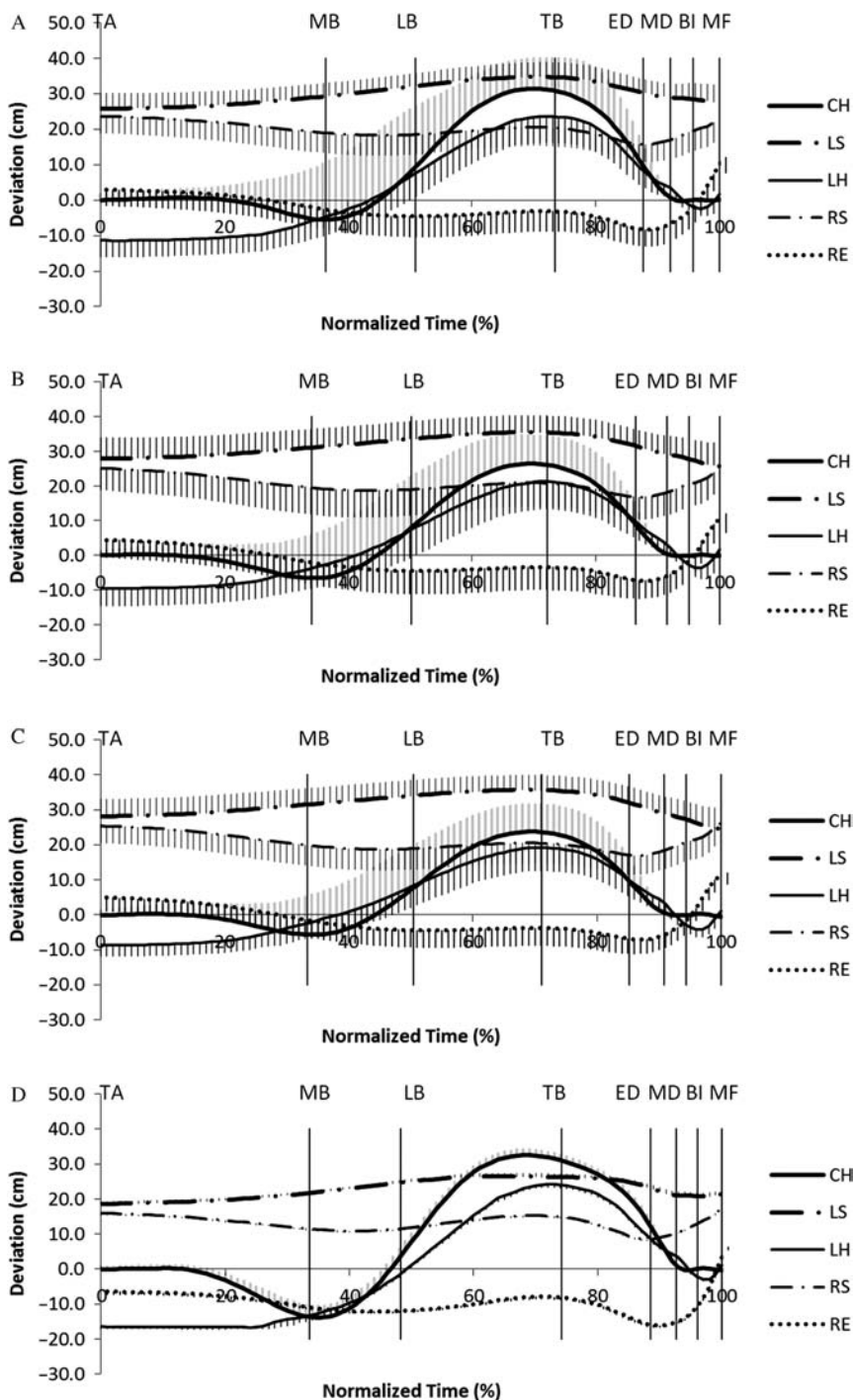
Figure 6. The off-plane motion patterns of the clubhead and shoulder/arm joints: the driver, 5-iron, and pitching wedge conditions for all participants ($n = 14$; A–C) and the driver condition for a participant ($n = 5$; D). Points: CH, clubhead; LS, left shoulder; LH, left hand; RS, right shoulder; and RE, right elbow. Events: TA, take-away; MB, mid backswing; LB, late backswing; TB, top of backswing; ED, early downswing; MD, mid downswing; BI, ball impact; and MF, mid follow-through.

shoulders. The relative inclinations and directions of inclination of the MPs were not as consistent as the slopes and direction angles of the FSP with the IGVs being 5.2° or less (relative inclination) and 7.2° or less (direction of inclination). The direction of inclination measures showed larger inter-golfer variability and IGV than the relative inclination measures.

The shoulder/arm points revealed vastly different relative motion patterns to the FSP from each other. Substantially larger mean relative inclinations were observed in the right shoulder and elbow (30–39°) than in the left shoulder and hand (10–15°), meaning that the left-arm points were moving more parallel to the FSP than their right-arm counterparts. More importantly, the shoulder/arm points revealed completely different direction of inclination profiles with the MPs of the left-arm points inclined forward ($\theta_{MP} > 0°$; Figure 5) but those of the right-side points inclined backward ($\theta_{MP} < 0°$; Table IV). The MPs of the shoulders ($|\theta_{MP}| < 90°$; inclined upward) were flatter than those of the left hand and right elbow ($|\theta_{MP}| > 90°$; inclined downward). The orientations of the MPs formed by the shoulder/arm points clearly show that the arm and shoulder girdle motions are not a single-plane motion as depicted in the multi-pendulum models (Cochran & Stobbs, 1968; Jorgensen, 1994; Sprigings & Neal, 2000).

The club effects on the orientations of the MPs were mainly observed in the left arm (Table IV). The relative orientations of the MPs of the right shoulder and elbow to the FSP were maintained across all clubs (approximately 30° of relative inclination and -76° of direction of inclination for the right shoulder and 38° and -106° for the elbow). In other words, as the FSP orientation changes with different clubs, the motions of the right shoulder and elbow are adjusted accordingly and the relative orientations of their MPs to the FSP remain unaltered. The left shoulder and hand, however, exhibited changes as the FSP orientation changes with different clubs. The changes in the direction of inclination were more notable than those in the relative inclination (Table IV). The left shoulder plane showed gradually more upward inclination as the club got shorter (driver → 5-iron → pitching wedge). The left-hand plane showed gradually more forward inclination as the club got shorter (Table IV).

Clubhead and body points exhibited large mean maximum deviations from the FSP (20.5–36.5 cm for the clubhead, shoulders, and hand; Table V) and generated significant off-plane motions (clubhead and hand in particular; Figure 6) during the swing. The IGVs of the maximum deviations from the FSP were 2.6 cm or less, showing high intra-golfer consistency in the skilled golfers. The shoulder points continuously stayed above the FSP while the right elbow stayed below for the most part of the swing. The right elbow, in general, stayed closer to the FSP than other points throughout the swing and at TA and BI in particular. This means that the glass pane that connects the clubhead and the right elbow (not the shoulder line used by Hogan & Wind, 1957) at TA is a good approximation of the FSP. At BI, the left hand and right elbow are closely aligned with the FSP, meaning that near the impact the clubshaft and right forearm also join the FSP (Figure 6).

Validity of the planar multi-pendulum models

From the profiles of the relative orientations of the MPs and the maximum deviations of the shoulder/arm points, it is evident that the planar swing assumption of the multi-pendulum models was an over-simplification. While the multi-pendulum models allow scientists and practitioners to understand how a high clubhead velocity can be developed through 'kinetic energy transfer' from the proximal lever to the distal (Cochran & Stobbs, 1968) and the importance of a 'delayed release' (Cochran & Stobbs, 1968; Sprigings & Mackenzie, 2002), they cannot incorporate the complex motions of the trunk, shoulder girdles, and arms. As a result of

Table V. Maximum deviation of the clubhead and shoulder/arm points from the functional swing plane (FSP) during the entire swing ($n = 14$; $M \pm SD$).

	Driver		5-Iron		Pitching wedge		Sig. effects
	Group mean	(IGV)	Group mean	(IGV)	Group mean	(IGV)	
Clubhead	35.1 ± 9.8	(1.8 ± 1.0)	29.6 ± 7.7[a]	(2.6 ± 2.1)	27.0 ± 8.0[a,b]	(2.4 ± 1.1)	
Left shoulder	35.0 ± 4.3	(0.8 ± 0.4)	36.0 ± 4.1	(1.3 ± 0.9)	36.5 ± 4.0[c]	(1.1 ± 0.6)	POINT
Left hand	24.4 ± 7.0[c,d]	(1.4 ± 0.8)	22.1 ± 6.9[a,c,d]	(2.0 ± 1.1)	20.5 ± 6.4[a,c,d]	(1.6 ± 0.8)	POINT × CLUB
Right shoulder	25.5 ± 5.4[c,d]	(0.8 ± 0.6)	27.0 ± 4.9[c]	(1.3 ± 0.7)	27.8 ± 4.8[a,c,d,e]	(1.0 ± 0.5)	
Right elbow	-8.9 ± 4.7[c,d,e,f]	(0.8 ± 0.5)	-7.4 ± 4.0[c,d,e,f]	(1.3 ± 1.0)	-7.1 ± 3.9[c,d,e,f]	(1.0 ± 0.7)	

Note: A positive maximum deviation means the point is positioned above the FSP, vice versa. Abbreviation: IGV, intra-golfer variability; [a] significantly different from the matching driver condition; [b] significantly different from the matching 5-iron condition; [c] significantly different from the matching clubhead condition; [d] significantly different from the matching left shoulder condition; [e] significantly different from the matching left hand condition; [f] Significantly different from the matching right shoulder condition.

the overwhelming popularity of the multi-pendulum models for over 40 years, important trunk/shoulder/arm motions such as lateral flexion of the trunk, elevation/depression and winging of the shoulder girdles, and flexion of the dominant elbow have been practically ignored in scientific research. Moreover, although the trunk rotation has received some attention (e.g. McTeigue et al., 1994; Burden et al., 1998; Lindsay et al., 2002; Egret et al., 2003; Myers et al., 2008), simple shoulder rotation projected to the ground was used in most cases, and the complex trunk motion (rotation and lateral flexion) is still not well understood. Complete body models that can incorporate a full array of trunk (including lateral flexion), shoulder (including elevation/depression and winging), and arm (including elbow flexion/extension) motions must be developed, and these motions must be the centerfold of future in-depth 3D golf swing studies.

Swing styles

A further analysis of the deviation patterns of the clubhead from the FSP revealed two different swing styles used by skilled golfers: semi-planar and spiral swing. The majority (12/14) of the participants were classified as 'semi-planar' swingers (Figure 7A) and two as 'spiral' swingers (Figure 7B). In the semi-planar swing, the FSP served as the lower boundary of the clubhead motion as golfers moved the clubhead down quickly toward the FSP during the transition phase (TB–MD) and executed a clean planar swing in the execution phase (MD–MF) before moving the clubhead back up in the late follow-through phase (Figure 7A). In the spiral swing style, however, the clubhead showed a helical trajectory in the execution phase. Golfers in this category moved the clubhead down gradually toward the FSP during the transition phase, but the clubhead crossed the FSP and moved further down during the execution phase and late follow-through. The spiral swing style was characterized by large clubhead deviations from the FSP at the beginning and end of the MD–MF phase (Figure 7B) and, as a result, the plane fitting errors of the spiral swingers ($n = 2$, RMS = 0.7 ± 0.1 cm, maximum = 2.1 ± 0.2 cm) were substantially larger than those of the semi-planar swingers ($n = 12$, RMS = 0.2 ± 0.1 cm, maximum = 0.7 ± 0.3 cm).

One notable difference between the two styles is the direction of the clubhead motion at the beginning of the downswing. While the clubhead accelerates moving toward the FSP
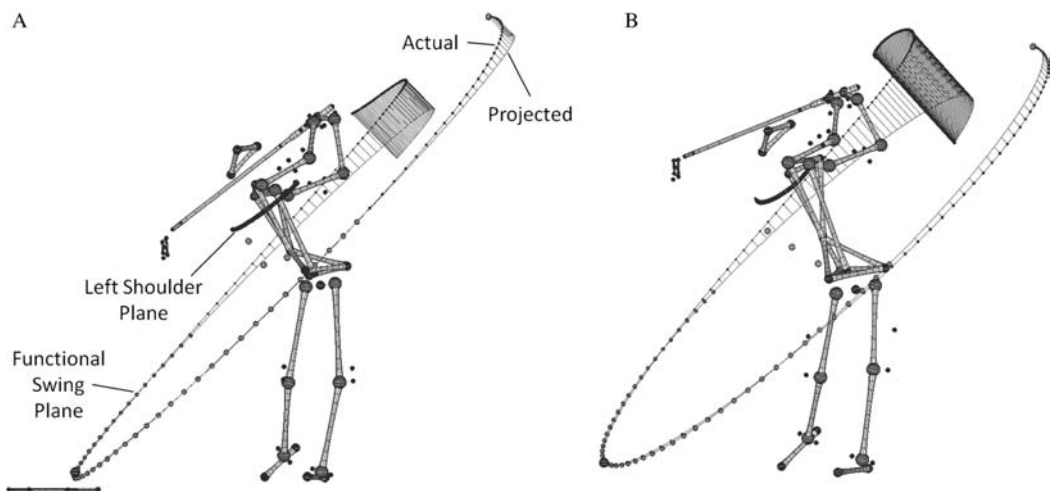

Figure 7. The downswing styles: (A) 'semi-planar' and (B) 'spiral'. The trajectory of the clubhead was projected to the FSP to visualize the direction and magnitude of the clubhead deviation from the FSP.

from the very beginning in the semi-planar swing, the clubhead initially moves slightly away from or parallel to the FSP in the spiral swing (Figure 7). This initial clubhead motion in the spiral swing style can make it more difficult to bring the clubhead down toward the FSP before the shaft reaches the MD position. It appears that the initial motion of the clubhead toward the FSP is an important prerequisite of a clean planar swing during the execution phase, but further investigations are necessary.

A spiral trajectory is essentially caused by a rotation around an axis and a translation along the axis, which means that two different forces act on the clubhead simultaneously: the on-plane force parallel to the FSP (such as the centripetal force) and the off-plane force perpendicular to the FSP. This additional off-plane force makes a spiral swing mechanically more complex than the semi-planar swing (with more room for errors/inconsistency), and one may speculate that the semi-planar swing is the superior swing style between the two. Further investigations on the issue of skill level (handicap) versus prevalent swing style and on the relationship between the swing style and biomechanical performance characteristics are warranted.

Trunk rotation and shoulder motion versus X-factor

One advantage of the FSP-based 3D analysis is that it can offer new insights into key contemporary golf coaching/science issues such as the X-factor. The torsional separation of the shoulder line from the hip line at the TB and in early downswing phase, X-factor/X-factor stretch (McLean, 1992; McTeigue et al., 1994; Cheetham et al., 2001), has often been related to the impact velocity, and the underlying mechanism has been explained mainly in the context of the 'stretch-shortening cycle' (e.g. Hume et al., 2005). Although some studies have reported inter-group (pros vs. pros, pros vs. amateurs, etc.) differences in the X-factor/X-factor stretch (McLean, 1992; McTeigue et al., 1994; Cheetham et al., 2001), research has failed to demonstrate a direct causal relationship between the X-factor/X-factor stretch and the clubhead velocity.

A forceful trunk rotation produced by pre-stretched trunk rotators due to a large X-factor may sound like a feasible cause of high impact velocity in the planar multi-pendulum perspective, but the findings of this study suggest otherwise. Since the MP of the left shoulder is inclined forward/upward ($\theta_{MP} < 90°$; Figure 5), a $10-15°$ relative inclination to the FSP makes the shoulder plane flatter (Table IV; Figure 5). The trunk plane (transverse) is also flatter than the FSP as the trunk axis (longitudinal) is aligned more upright than the normal axis of the FSP (Figure 7). The trunk rotation and linear shoulder motion during the downswing/follow-through, therefore, tend to promote an off-plane motion of the clubhead (and a spiral swing) by pulling it down past the FSP. The relative orientations of the shoulder MP and trunk plane to the FSP and the curvature of the clubhead trajectory with respect to the FSP (in the semi-planar swing in particular) suggest that trunk rotation is not what drives the downswing and the arms move somewhat independently of the trunk in a fashion to secure a clean planar motion of the clubhead during the execution phase. Therefore, it is an unlikely scenario that a forceful trunk rotation directly generates a high impact velocity.

The hand and clubhead motions during a downswing are produced by the combined efforts of the arms (shoulder and elbow joint motions), shoulder girdles (elevation/depression and winging), and trunk (rotation and lateral flexion). The position of the shoulder line with respect to the pelvis line at TB (X-factor) can affect the subsequent motions of the arms, shoulder girdles, and trunk (i.e. the motion paths of the hands and clubhead) and ultimately the FSP. Therefore, the difference in the X-factor/X-factor stretch among different skill groups may mean some fundamental differences in the swing technique (FSP, MPs, etc.),

which can then affect the clubhead velocity. Further investigations on biomechanically correct meanings of the X-factor/X-factor stretch are warranted to better explain the causal relationship between the X-factor and impact velocity/shot distance, if any.

Popular swing models: on-plane, one-plane, and two-plane swing

The FSP-based 3D analysis also allows a mechanical scrutiny of popular swing models such as Hank Haney's 'On-Plane' swing (Haney & Huggan, 1999) and Jim Hardy's 'One-Plane' and 'Two-Plane' swings (Hardy & Andrisani, 2005). In the On-Plane swing model, the clubshaft remains parallel to the original shaft plane (the plane formed by the clubshaft and the target line at address) from start to finish and the club must return to the address position at BI. Mechanically speaking, the On-Plane swing is a poor model because moving the club through multiple planes while maintaining the shaft angle causes a spiral trajectory throughout the entire swing. The golfer must deal with two different forces (the on-plane force parallel to the shaft plane and the off-plane force perpendicular to the shaft plane) simultaneously and it is almost impossible to maintain the shaft parallel to the original plane during the downswing (<260 ms) due to the inertia of the fast-moving clubhead. The On-Plane motion appears to be possible only in a series of still postures. Figure 6 shows that the left hand is initially located below the FSP at TA but returns close to the FSP at BI. The shaft also stays almost parallel to the FSP during the ED–MD phase (similar clubhead and left-hand deviations from the FSP) but on the FSP during the execution phase (close-to-zero deviations). The clubshaft returns not to the address position but to the FSP. Although keeping the clubshaft parallel to the original plane for the entire swing sounds attractive, it is neither healthy mechanically nor natural anatomically. The original shaft plane is flatter than the FSP, so a true On-Plane swing only promotes a severe spiral swing.

Jim Hardy classified swings into two types based on the alignment of the leading (left) arm with respect to the shoulder line at TB along with the degree of trunk bending: One-Plane and Two-Plane (Hardy & Andrisani, 2005). In the One-Plane swing, a golfer swings the arms and the club around the bent-over spine to the same plane (shoulder line) during the backswing. In the Two-Plane swing, the trunk is positioned more upright than the One-Plane swing and the leading arm is positioned more upright than the shoulder line at TB. First, Hardy's fundamental view of the swing (the combination of a circular motion about the trunk axis and an up-and-down motion along the trunk axis of the arms and club) generates a helical trajectory, not a plane. As shown in Figure 7, the clubhead motion is fairly independent of the trunk rotation, forming a clean planar trajectory in the execution phase. Second, due to the 2D perspective, the same relative position of the arm to the shoulder line at TB can be perceived differently depending on the amount of trunk rotation during the backswing. Therefore, the alignment/misalignment of the arm to the shoulder line at TB may not mean any fundamentally different backswing motions (one plane vs. two planes). Third, a downswing can be divided into the transition and execution phases and alignment/misalignment of the arm to the shoulder line may affect the transition phase, but not the execution phase. Fourth, the shoulder girdle motion is not as simple as a rotation about the trunk axis, evidenced by the vastly different MPs formed by the two opposing shoulder points (Figure 4; Table IV).

Limitation

One limitation of this study was that foam practice balls, not actual golf balls, were used in an indoor biomechanics laboratory. While participants reported no abnormal feel from hitting

the foam balls, it is certainly possible for the clubhead motion immediately after the impact to be altered by the ball used.

Conclusion

The purpose of this study was to determine the FSP of the clubhead and the MPs of the key pendulum points (shoulders, left hand, and right elbow) that characterize a golfer's fundamental downswing motion, and to systematically assess planarity of the golf swing based on the FSP and the MPs. For this, the FSPs were obtained from the MD–MF phase, and the relative orientations of the MPs to the FSP were computed along with the deviations of the clubhead and shoulder/arm points from the FSP.

From the findings of the study, the following conclusions were derived:

- Skilled golfers exhibited well-defined and consistent FSPs and longer clubs generated flatter and more closed swing planes with respect to the target. The downswing could be divided into two distinct phases: the transition phase (top of backswing to mid downswing) and the planar execution phase (mid downswing to mid follow-through). The downswing was planar at least during the execution phase, the most important phase of a golf swing.
- Skilled golfers exhibited reasonably well-defined and consistent MPs of the shoulders, left hand, and right elbow with left hand and right elbow showing less planar motion trajectories than the shoulders. The shoulder/arm points moved on vastly different MPs from each other and the right shoulder and right elbow were characterized by consistent relative motions to the FSP across different clubs.
- The shoulder/arm points also exhibited large deviations from the FSP.
- The planar swing assumption of the multi-pendulum swing models is an over-simplification and is not appropriate for an in-depth understanding of the golf swing.
- The semi-planar swing style was identified as the typical swing style among the skilled golfers.

References

Andriacchi, T. P., Andersson, G. B. J., Fermier, R. W., Stern, D., & Galante, J. O. (1980). A study of lower-limb mechanics during stair climbing. *The Journal of Bone and Joint Surgery*, *62A*, 749–757.
Bell, A. L., Pedersen, D. R., & Brand, R. A. (1990). A comparison of the accuracy of several hip center location prediction methods. *Journal of Biomechanics*, *23*, 617–621.
Budney, D. R., & Bellow, D. G. (1979). Kinetic analysis of a golf swing. *Research Quarterly*, *50*, 171–179.
Burden, A. M., Grimshaw, P. N., & Wallace, E. S. (1998). Hip and shoulder rotations during the golf swing of sub-10 handicap players. *Journal of Sports Sciences*, *16*, 165–176.
Campbell, K. R., & Reid, R. E. (1985). The application of optimal control theory to simplified models of complex human motions: the golf swing. In D. A. Winter, R. W. Norman, R. P. Wells, K. C. Hayes, and A. E. Patla (Eds.), *Biomechanics IX-B* (pp. 527–532). Champaign, IL: Human Kinetics Publishers.
Cheetham, P. J., Martin, P. E., Mottram, R. E., & St Laurent, B. F. (2001). The importance of stretching the 'X-factor' in the downswing of golf: the 'X-Factor stretch'. In P. R. Thomas (Ed.), *Optimising performance in golf* (pp. 192–199). Brisbane, QLD: Australian Academic Press.
Cochran, A., & Stobbs, J. (1968). *The search for the perfect swing*. Philadelphia, PA: J.B. Lippincott.
Coleman, S., & Anderson, D. (2007). An examination of the planar nature of golf club motion in the swings of experienced players. *Journal of Sports Sciences*, *25*, 739–748.
Coleman, S., & Rankin, A. (2005). A three-dimensional examination of the planar nature of the golf swing. *Journal of Sports Sciences*, *23*, 227–234.
Egret, C. I., Vincent, O., Weber, J., Dujardin, F. H., & Chollet, D. (2003). Analysis of 3D kinematics concerning three different clubs in golf swing. *International Journal of Sports Medicine*, *24*, 465–469.

Haney, H., & Huggan, J. (1999). *The only golf lesson you'll ever need: Easy solutions to problem golf swings*. New York: HarperCollins.

Hardy, J., & Andrisani, J. (2005). *The plane truth fro golfers: Breaking down teh one-plane swing and the two-plane swing anf finding the one that's right for you*. New York: McGraw-Hill.

Hogan, B., & Wind, H. W. (1957). *Ben Hogan's five lessons: The modern fundamentals of golf*. New York: Simon & Schuster.

Hume, P. A., Keogh, J., & Reid, D. (2005). The role of biomechanics in maximising distance and accuracy of golf shots. *Sports Medicine*, 35, 429–449.

Jorgensen, T. (1994). *The physics of golf*. New York: American Institute of Physics Press.

Lampsa, M. A. (1975). Maximizing distance of the golf drive: An optimal control study. *Journal of Dynamic Systems, Measurements, and Controls: Transactions of ASME*, 97G, 362–367.

Lindsay, D. M., Horton, J. F., & Paley, R. D. (2002). Trunk motion of male professional golfers using two different golf clubs. *Journal of Applied Biomechanics*, 18, 366–373.

MacKinnon, C. D., & Winter, D. A. (1993). Control of whole body balance in the frontal plane during human walking. *Journal of Biomechanics*, 26, 633–644.

McLean, J. (1992). Widen the gap. *Golf Magazine*, 1992 (12), 49–53.

McTeigue, M., Lamb, S. R., Mottram, R., & Pirozzolo, F. (1994). Spine and hip motion analysis during the golf swing. In A. J. Cochran, and M. R. Farrally (Eds.), *Science and golf II: Proceedings of the World Scientific Congress of Golf* (pp. 50–58). London: E & FN Spon.

Milburn, P. D. (1982). Summation of segmental velocities in the golf swing. *Medicine and Science in Sports and Exercise*, 14, 60–64.

Milne, R. D., & Davis, J. P. (1992). The role of the shaft in the golf swing. *Journal of Biomechanics*, 25, 975–983.

Myers, J., Lephart, S., Tsai, Y. S., Sell, T., Smoliga, J., & Jolly, J. (2008). The role of upper torso and pelvis rotation in driving performance during the golf swing. *Journal of Sports Sciences*, 26 (2), 181–188.

Neal, J. R., & Wilson, B. D. (1985). 3D kinematics and kinetics of the golf swing. *International Journal of Sport Biomechanics*, 1, 221–232.

Nesbit, S. M. (2005). A three dimensional kinematic and kinetic study of the golf swing. *Journal of Sports Science and Medicine*, 4, 499–519.

Pickering, W. M., & Vickers, G. T. (1999). On the double pendulum model of the golf swing. *Sports Engineering*, 2, 161–172.

Press, W. H., Teukolsky, S. A., Vetterling, W. T., & Flannery, B. P. (2002). *Numerical recipes in C++: The art of scientific computing* (2nd ed.). Cambridge, England: Cambridge University Press.

Sanders, R. H., & Owens, P. C. (1992). Hub movement during the swing of elite and novice golfers. *International Journal of Sport Biomechanics*, 8, 320–330.

Sprigings, E. J., & Mackenzie, S. J. (2002). Examining the delayed release in the golf swing using computer simulation. *Sports Engineering*, 5, 23–32.

Sprigings, E. J., & Neal, R. J. (2000). An insight into the importance of wrist torque in driving the golfball: A simulation study. *Journal of Applied Biomechanics*, 16, 356–366.

Tylkowski, C. M., Simon, S. R., & Mansour, J. M. (1982). Internal rotation gait in spastic cerebral palsy. *The Hip: Proceedings of the 10th Open Meeting of the Hip Society*, 10, 89–125.

Vaughan, C. L. (1981). A three-dimensional analysis of the forces and torques applied by a golfer during the downswing. In A. Morecki, K. Fidelus, K. Kedzior, and A. Witt (Eds.), *Biomechanics VII-B*. Baltomore, MD: University Park Press.

Williams, D. (1967). The dynamics of the golf swing. *The Quarterly Journal of Mechanics and Applied Mathematics*, 20 (2), 247–264.

Williams, K. R., & Sih, B. L. (2002). Changes in golf clubface orientation following impact with the ball. *Sports Engineering*, 5, 65–80.